IMAGE-BASED MEASUREMENT OF CARGO TRAFFIC FLOW IN COMPLEX NEURITE NETWORKS

Xiaoqi Chai[1], *Douglas Qian*[1], *Qinle Ba*[1], *Angran Li*[2], *Yongjie Jessica Zhang*[1,2], *and Ge Yang*[1,3]
[1]Department of Biomedical Engineering; [2]Department of Mechanical Engineering; [3]Department of Computational Biology, Carnegie Mellon University, Pittsburgh, PA 15213, USA

ABSTRACT

Neurons depend critically on active transport of cargoes throughout their complex neurite networks for their survival and function. Defects in this process have been strongly associated with many human neurodevelopmental and neurodegenerative diseases. To understand related neuronal physiology and disease mechanisms, it is essential to measure the traffic flow within the neurite networks. Currently, however, image analysis methods required for this measurement are lacking. To address this deficiency, we developed a method that could measure the flow rates of cargo traffic at any specified locations along individual branches of the neurite networks. Our method is based on detecting and counting cargo trajectories passing through the specified locations of measurement in kymographs, which are spatiotemporal maps of cargo movement within one-dimensional neurites. A main focus of our method development is robust performance, which ensures that our method works reliably and accurately under low signal-to-noise ratios. We validated and benchmarked our method using both synthetic and actual image data and found its accuracy to be >85% on average under normal conditions. Our method can be used to measure traffic flow in not just neurite networks but also other intracellular networks such as cytoskeletal filament networks.

Index Terms— kymograph, neurite network, traffic flow, network flow, image-based measurement

1. INTRODUCTION

Neurons build highly complex and branched networks of neurites, i.e. axons and dendrites, to carry out their information processing functions and to form neural circuits (Fig. 1) [1]. However, the network geometry creates a significant transportation challenge because to survive and function, neurons must transport a wide variety of essential materials packaged in different forms of cargoes, such as membranous organelles, throughout the networks [2]. Dysfunction of this transport process has been closely associated with a wide range of human neurodevelopmental diseases, such as autism [3], and neurodegenerative diseases, such as Alzheimer's disease [4]. To understand how the transport process is conducted in healthy neurons and how transport defects develop under disease conditions, it is essential to quantitatively measure traffic flow in the neurite networks. For example, neurons must balance cargo traffic to avoid either traffic jams or cargo shortage in individual neurite branches. To understand how this balance is achieved, quantitative measurements of cargo traffic flow in individual neurite branches are required.

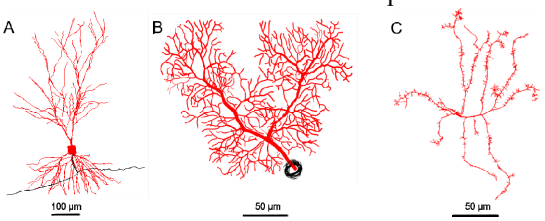

Figure 1. Selected examples of complex geometry of neurite networks. All examples are from the NeuroMorpho database [5]. Soma and axons: black; dendrites: red. (a) Rat pyramidal neuron (NMO_00218) (b) Mouse cerebellum Purkinje neuron (NMO_35058) (c) Drosophila multidendritic-dendritic arborization class III neuron (NMO_06962)

Various image analysis methods have been developed for characterizing cargo traffic in a single neurite [6-10]. A common feature of these methods is that they are all based on kymographs, which are intuitive and effective representations of spatiotemporal patterns of cargo movement. Another common feature of these methods is that they all aim to recover complete cargo trajectories for comprehensive characterization of cargo behavior. For example, Mukherjee and colleagues developed an automated method [7] that recovered complete trajectories of secretory granules transported in the axon by detecting the corresponding curves in kymographs using the mini-cover approach [11]. A similar strategy was used by Welzel and colleagues for recovering complete trajectories of cargoes transported in the axon [9], except that they used the Hough transform to detect curves in kymographs. Overall, however, because these methods are designed for a single neurite, they generally are not suitable for measuring traffic in the neurite networks, given their complex and branched geometry.

In this study, our goal is to measure the traffic flow rate, which we define as the average number of cargoes passing through a specified location of measurement over a unit period of time. To measure this rate, we only need knowledge of cargo movement through the specified location, not complete cargo trajectories. Therefore, we developed a method that counted the number of trajectories

passing specified locations of measurement in kymographs. A main focus of our method development is robustness so that our method works reliably and accurately under low signal-to-noise ratios (SNRs). Specifically, in this study, we adopt the definition of SNR as $SNR = \left(\mu_{signal} - \mu_{background}\right) / \sigma_{background}$ where μ_{signal} denotes the mean of signal, while $\mu_{background}$ and $\sigma_{background}$ denote the mean and standard deviation of background, respectively. We validated and benchmarked our method using synthetic and real images and confirmed that it could achieve >85% accuracy on average. The method we developed can be used to measure cargo traffic in not only neurite networks but also other intracellular networks, such as cytoskeletal filament networks.

2. METHODS

2.1 Overview of workflow

Figure 2 shows the overall workflow of our method. Time-lapse images of cargo transport in a neurite network are aligned to remove image drift if necessary and then added up to produce a single sum image. From the sum image, geometry of the neurite network is extracted manually or semi-automatically using the neurite tracing function in the TREES toolbox [12]. Extracted network geometry is represented and stored using the data structure for neurite networks in the TREES toolbox [12]. Then, locations for measurement of traffic flow are specified manually or automatically. For those neurites that contain specified locations, kymographs are generated as described in [7], except that they may span multiple connected neurites (see e.g. Fig. 3A). The computational background removal algorithm described in [13] is applied to the kymographs to reduce the level of background fluorescence and to remove trajectories of stationary cargoes. After background removal, the Steger's algorithm for curve detection [14] is used to detect cargo trajectories. Lastly, the number of trajectories passing through the specified locations of measurement in both anterograde (i.e. away from cell body) and retrograde (i.e. towards cell body) directions are counted, and the calculated flow rates are exported.

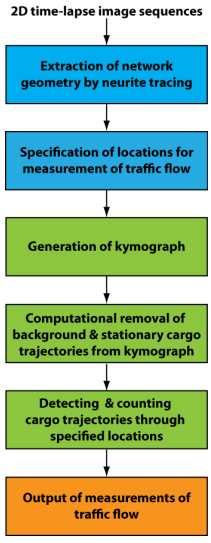

Figure 2. Overview of workflow

2.2 Experimental data collection

In this study, we used primarily time-lapse movies of transport of APP (amyloid precursor protein) vesicles in cultured rat hippocampal neurons for developing, validating and benchmarking our method. Hippocampal neuron were dissociated from dissected hippocampi (BrainBits) and cultured in Neurobasal media containing B27 supplement and 2.5 mM GlutaMAX-I (Gibco). Neurons were transfected with APP-YFP plasmids, a gift of Dr. Carlos Dotti from the Katholieke Universiteit Leuven, using Lipofectamine 2000 (Invitrogen). Time-lapse movies of APP vesicles were collected at 10 frame per second on a Nikon Eclipse Ti-E inverted microscope with a CoolSNAP HQ2 camera (Photometric) and a 100×/1.40NA oil objective lens. During imaging, cells were maintained in a Tokai Hit stage incubator at 37 °C with 5% CO_2. The effective pixel size was 0.0645 μm.

2.3 Computational removal of background and stationary cargo trajectories

A commonly encountered problem in analyzing cargo traffic in neurite branches is the high level of background fluorescence (Fig. 3A), which leads to high levels of background and low SNRs in kymographs (Fig. 3B). To resolve this problem, we applied the computational background removal algorithm described in [13] to the kymographs. The removal process served two purposes. First, it reduced the background fluorescence level and increased the SNR (Fig. 3C). For example, the kymograph in Fig. 3B had an SNR of 4.7. After background removal, the SNR was increased to 7.0 (Fig. 3C). Second, it removed trajectories of stationary cargoes (Fig. 3D) and, therefore, simplified subsequent detection and analysis of trajectories of moving cargoes. Overall, we found this background removal process to be essential to robustness of our method under low SNRs.

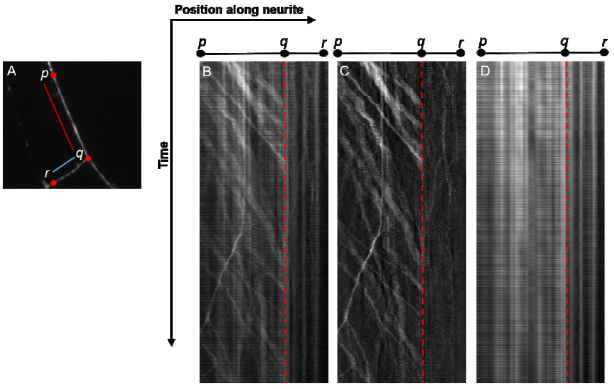

Figure 3. Kymograph background removal. (A) A representative neurite junction, a basic element of the neurite network structure. (B) Raw kymograph over *pq* and *qr* before background removal. (C) Kymograph after background removal. (D) Removed background, including stationary cargo trajectories.

2.4 Detecting and counting cargo trajectories

Following background removal, we detected cargo trajectories in the kymograph using the Steger's curve

detection algorithm [14]. As noted by previous studies of cargo transport in a single neurite [6-10], curve detected from kymographs are often fragmented (Fig. 4C) because of factors such as noise, cargo moving out of focus, etc. If the goal is to recover complete cargo trajectories, the trajectory segments must be linked. However, it is known that performance of this linking process degrades substantially under low SNRs [15]. Since measurement of traffic flow does not require complete trajectories, we developed a method that did not require linking of trajectory segments.

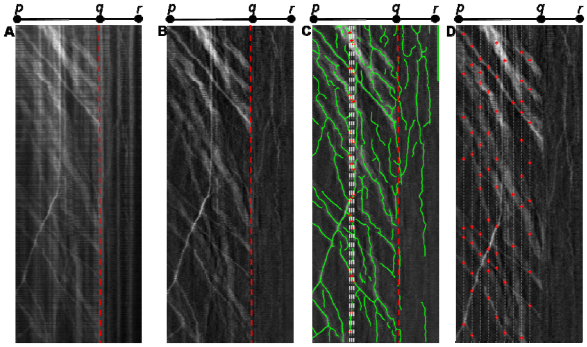

Figure 4. Cargo trajectory detection and counting. (A) Raw kymograph, same as Fig. 3B (B) Kymograph after background removal, same as Fig. 3C. (C) Detected trajectories are shown in green and overlaid onto the kymograph in (B). (D) A total of 9 equally spaced locations are specified between *pq* for traffic flow measurement. The locations are indicated by the white dotted lines. The red markers indicate passages of trajectory segments in both directions through the dotted lines.

Taking the kymographs shown in Fig. 3A-B or Fig. 4A-B as an example, a specified location of measurement corresponds to a vertical line in the kymograph (see e.g. the white dashed lines in Fig. 4C and the white dotted lines in Fig. 4D). The numbers of cargoes passing through the specified location in the anterograde and retrograde direction can be determined by counting the trajectories passing the vertical line accordingly. However, the trajectories may be fragmented at the position of the vertical line. To enhance the robustness of our method, we developed a sliding-window strategy to suppress the fluctuation in flow rate measurement caused by the fragmentation. Specifically, instead of counting the trajectories only at the specified location, we repeated this counting process at a distance d to both the left and the right of the location p (Fig. 4C). The total width of the window of measurement was therefore $2d+1$. Consequently, we would obtain three readouts of cargo number for each trajectory, at positions p-d, p, p+d, respectively. We then took their median as the final measurement. In this way, if the gap of the trajectory was less than $2d$, a correct readout could still be obtained even if the trajectory was broken at p. We found that this strategy effectively increased the accuracy of traffic flow measurement because the traffic flow usually remained steady within the measurement widow as long as the width was small enough. In practice, we typically set d to be 5 pixels.

3. RESULTS

3.1. Experiments using synthetic images

To test our method, we generated synthetic images of cargo transport in a single neurite under different SNRs (Fig. 5A-C) and spatial densities (Fig. 5D-F). Our simulation was designed to match the experimental imaging settings described in Section 2.1. For a proof of principle, we simulated cargoes to move at largely constant velocities without pausing or switching in directions (Fig. 5A-F). We define measurement accuracy as

$$Accuracy = \left(1 - \left|N_{Measured} - N_{Groundtruth}\right| / N_{Groundtruth}\right) \times 100\%,$$

where $N_{Groundtruth}$ is the ground-truth number of cargoes passing a specific location of observation. $N_{Measured}$ is the number of cargoes counted by our method.

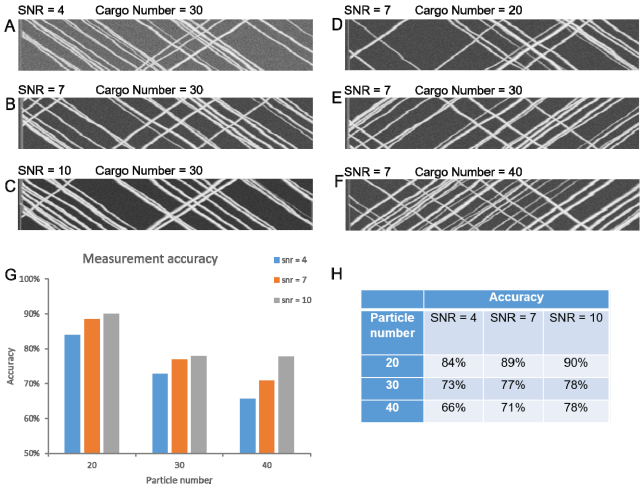

Particle number	Accuracy		
	SNR = 4	SNR = 7	SNR = 10
20	84%	89%	90%
30	73%	77%	78%
40	66%	71%	78%

Figure 5. Experimental results using synthetic images. (A-C) Representative kymographs generated from synthetic images. Cargo number was kept at 30. SNR was varied from 4 to 7. (D-F) SNR was kept at 7, cargo number was varied from 20 to 40. (G) A bar plot comparing measurement accuracies under different conditions. (H) A table listing measurement accuracies under different conditions.

Overall, we found that under the same spatial density, increasing SNRs led to increases in measurement accuracy, as expected (Fig. 5G-H). However, under the same SNR, increases in spatial density led to decreases in measurement accuracy decreases (Fig. 5G-H). The Steger's curve detection algorithm uses an isotropic Gaussian filter with $\sigma \geq w/\sqrt{3}$ where w is the maximum width of curves to be detected. We found that a main reason for the reduced accuracy under high spatial densities was that curves close to each were merged after the isotropic filtering.

3.2 Experiments using real images

To further test our method, we also used it to analyze real image data. Here we present results for the example shown in Figure 4. We determined the ground-truth cargo numbers by manual counting. Overall, we conducted measurements at 9 locations, with a spacing of 20 pixels, or 1.29 μm (Fig. 4D). Because the vast majority of cargoes in this case moved towards the right of the kymograph, which was in the anterograde direction, we benchmarked accuracy of our method only in this direction.

Table 1. Summary of results for the example in Figure 4.

Observation Location	Groundtruth count	Algorithm count	Accuracy
20	10	8	80%
40	10	9	90%
60	9	10	89%
80	9	8	89%
100	9	8	89%
120	8	4	50%
140	8	5	63%
160	9	9	100%
180	9	10	89%

We found that the accuracy in most cases was at ~90% but decreased substantially in two cases. We found that the performance degradation in these two cases was caused by two factors. First, some very weak trajectories were not detected by the Steger's algorithm. Second, convergence of multiple trajectories led to an increased counting error. We have also tested our method on multiple other datasets (result not shown). Overall, we found the accuracy of our method to be >85% on average.

3.3 Generating synthetic images for complex neurite networks

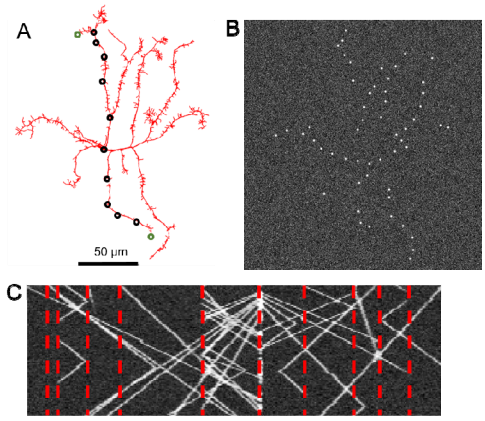

Figure 6. Generating synthetic images of cargo transport in a neurite network (A) Network geometry used for generating synthetic images, same as Fig. 1C. (B) A representative frame of generated synthetic images. (C) A kymograph was generated along the connected neurites from top to bottom between the two green circles shown in (A). Red dotted lines correspond to junctions marked by black circles in (A).

We have thus far tested our method under relatively simple neurite geometry. To further test our method over entire neurite networks, we generated synthetic images based on actual geometry of neurons retrieved from the NeuroMorpho database [5]. Figure 6 shows an example. For simplification, cargoes were simulated to move at constant velocities (Fig. 6C). Our method can be used to measure traffic flow not just within individual neurite branches but also over different branches.

4. CONCLUSIONS

In this study, we developed a method that measures traffic flow rates at any specified locations in complex neurite networks. To ensure robust performance under low SNRs, we used two strategies. First, we applied our computational background removal algorithm to improve SNRs [13]. Second, we used a sliding-window in counting trajectories to resolve at least partially the issue of fragmentation in trajectory detection. We tested our method using both synthetic and real image data and found that on average it achieved >85% accuracy. Our method also has its limitations. First, its accuracy may drop substantially in some cases (see e.g. Table 1). We are systematically documenting such cases, some of which are discussed in Section 3.2. Our goal is to optimize our method specifically to resolve such cases. Second, our method depends critically on the performance of the Steger's curve detection algorithm, whose performance degrades when the spatial density of trajectories is high due to its design to use a large isotropic Gaussian kernel for image filtering [14]. We are investigating different image filtering and curve detection algorithms to overcome this limitation.

Because our method requires only kymograph representation of cargo transport and does not depend on specific properties of cargo traffic in neurites, it is not restricted to neurite networks in its applications. Instead, it can be used to measure traffic flow along other one-dimensional structures, such as cytoskeletal filaments.

5. ACKNOWLEDGEMENTS

X.C. acknowledges a Ji-Dian Liang Graduate Research Fellowship. Y.J.Z. acknowledges NSF Faculty Career grant OCI-1149591. G.Y. acknowledges NSF Faculty Career grant DBI-1149494. Y.J.Z. and G.Y. also acknowledge a CMU Department of Mechanical Engineering seed grant for this project.

6. REFERENCES

[1] L. Luo, *Principles of Neurobiology*: Garland Science, 2015.

[2] C. I. Maeder, K. Shen, and C. C. Hoogenraad, "Axon and dendritic trafficking," *Current Opinion in Neurobiology,* vol. 27, pp. 165-170, 2014.

[3] V. Martínez-Cerdeño, "Dendrite and spine modifications in autism and related neurodevelopmental disorders in patients and animal models," *Developmental Neurobiology,* p. 10.1002/dneu.22417, 2016.

[4] V. A. Kulkarni and B. L. Firestein, "The dendritic tree and brain disorders," *Molecular and Cellular Neuroscience,* vol. 50, pp. 10-20, 2012.

[5] G. A. Ascoli, D. E. Donohue, and M. Halavi, "NeuroMorpho.Org: a central resource for neuronal morphologies," *Journal of Neuroscience,* vol. 27, pp. 9247-9251, 2007.

[6] N. Chenouard, J. Buisson, I. Bloch, P. Bastin, and J. C. Olivo-Marin, "Curvelet analysis of kymograph for tracking bi-directional particles in fluorescence microscopy images," in *2010 IEEE International Conference on Image Processing*, 2010, pp. 3657-3660.

[7] A. Mukherjee, B. Jenkins, C. Fang, R. J. Radke, G. Banker, and B. Roysam, "Automated kymograph analysis for profiling axonal transport of secretory granules," *Medical Image Analysis,* vol. 15, pp. 354-367, 2011.

[8] K. Zhang, Y. Osakada, W. Xie, and B. Cui, "Automated image analysis for tracking cargo transport in axons," *Microscopy Research and Technique,* vol. 74, pp. 605-613, 2011.

[9] O. Welzel, J. Knörr, A. M. Stroebel, J. Kornhuber, and T. W. Groemer, "A fast and robust method for automated analysis of axonal transport," *European Biophysics Journal,* vol. 40, pp. 1061-1069, 2011.

[10] M. Qiu, H.-C. Lee, and G. Yang, "Nanometer resolution tracking and modeling of bidirectional axonal cargo transport," in *2012 9th IEEE International Symposium on Biomedical Imaging (ISBI)* 2012, pp. 992-995.

[11] P. Felzenszwalb and D. McAllester, "A Min-Cover Approach for Finding Salient Curves," in *2006 Conference on Computer Vision and Pattern Recognition Workshop (CVPRW'06)*, 2006, pp. 185-185.

[12] H. Cuntz, F. Forstner, A. Borst, and M. Häusser, "The TREES toolbox—probing the basis of axonal and dendritic branching," *Neuroinformatics,* vol. 9, pp. 91-96, 2011.

[13] H.-C. Lee and G. Yang, "Computational removal ofbackground fluorescence for biological fluorescence microscopy," in *2014 IEEE 11th International Symposium on Biomedical Imaging (ISBI)* 2014, pp. 205-208.

[14] C. Steger, "An Unbiased Detector of Curvilinear Structures," *IEEE Trans. Pattern Anal. Mach. Intell.,* vol. 20, pp. 113-125, 1998.

[15] N. Chenouard, I. Smal, F. de Chaumont, M. Maska, I. F. Sbalzarini, Y. Gong*, et al.*, "Objective comparison of particle tracking methods," *Nat Meth,* vol. 11, pp. 281-289, 2014.